

This is the final peer-reviewed accepted manuscript of:

M. Mohammadgholiha, F. Zonzini and L. De Marchi, "Enabling Spatial Multiplexing in Guided Waves-based Communication: the case of Quadrature Amplitude Modulation realized via Discrete Frequency Steerable Acoustic Transducers," *2022 IEEE International Ultrasonics Symposium (IUS)*, 2022, pp. 1-4, doi: 10.1109/IUS54386.2022.9958829.

The final published version is available online at: [10.1109/IUS54386.2022.9958829](https://doi.org/10.1109/IUS54386.2022.9958829)

Rights / License:

The terms and conditions for the reuse of this version of the manuscript are specified in the publishing policy. For all terms of use and more information see the publisher's website.

*This item was downloaded from IRIS Università di Bologna (<https://cris.unibo.it/>)*

***When citing, please refer to the published version.***

# Enabling Spatial Multiplexing in Guided Waves-based Communication: the case of Quadrature Amplitude Modulation realized via Discrete Frequency Steerable Acoustic Transducers

Masoud Mohammadgholiha  
DEI-Department of Electrical,  
Electronic and Information Engineering  
University of Bologna, Italy  
m.mohammadgholiha@unibo.it

Federica Zonzini  
ARCES - Advanced Research  
Center on Electronic Systems  
University of Bologna, Italy  
federica.zonzini@unibo.it

Luca De Marchi  
DEI-Department of Electrical,  
Electronic and Information Engineering  
University of Bologna, Italy  
l.demarchi@unibo.it

**Abstract**—Guided Waves (GWs) communication using conventional transducers, e.g., PZT, encounters quite a few problems, such as complex hardware systems and waves multipath interference. To overcome such drawbacks, Frequency Steerable Acoustic Transducers (FSATs) which benefit from inherent directional capabilities can be fruitfully adopted to implement a spatial multiplexing strategy. The FSATs work on the frequency-dependent spatial filtering effect to generate/receive waves, resulting in a direct relationship between the direction of propagation and the frequency content of the transmitted/received signals. Thanks to this unique frequency-steering capability, FSATs are best suited to implement frequency-driven modulation protocols, such as the ones typically exploited for GWs-based data communication. Among these, the Quadrature Amplitude Modulation (QAM) scheme is advantageous in terms of noise immunity. Thus, the objective of this work is to combine QAM with the built-in spatial multiplexing capabilities of FSATs to realize, in hardware, frequency directivity, like the solutions that are currently being investigated in 5G communications.

**Index Terms**—Acoustic Data Communications, Frequency Steerable Acoustic Transducers, Quadrature Amplitude Modulation

## I. INTRODUCTION

Enabling digital data communication in a structural health monitoring (SHM) system is crucial for many industrial applications, where the acquired information about defects is needed to be transmitted from different locations [1], [2]. Such SHM systems typically rely on either wired or radio frequency (RF) wireless communications, which are not suitable for harsh environments where light propagation is very low [3]. Ultrasonic guided waves (GWs) have become a prominent alternative solution for acoustic data communication across a solid channel since they propagate over large distances within a structure with minimal attenuation and loss [4].

The implementation of acoustic data communication using GWs is generally performed through a number of Piezoelectric transducers (PZT) [5]. However, in this PZT networked systems, multi-mode propagation and reflections hinder the development of robust communication. To tackle such lim-

itations, Frequency Steerable Acoustic Transducers (FSATs) which benefit from inherent directional capabilities can be implemented [6]. In principle, the FSATs are based on a frequency-dependent spatial filtering effect, leading to a direct relationship between the direction of propagation and the frequency spectrum of the actuated/sensed signal [7]. Therefore, the FSATs eliminate the potential for multi-path interference, unlike conventional transducers which experience multiple arrivals of the same transmitted waveform. Furthermore, the spatial filtering of the FSATs minimizes the ringing and dispersion effects.

In this paper, a novel FSAT is designed for acoustic data communication in three different directions. Among the communication schemes, the Quadrature Amplitude Modulation (QAM) [8] is taken into account and combined with the inherent spatial multiplexing capabilities of FSATs to implement the frequency directivity.

## II. FREQUENCY STEERABLE ACOUSTIC TRANSDUCERS

According to the theory presented in [9], the voltage  $V_p(\omega)$  generated by an arbitrary shape patch  $\Omega_p(x, y)$  where there is a plane Lamb wave propagating at angle  $\theta$  can be represented as:

$$V_p(\omega) = jU(\omega)K_0(\omega)H(\theta)D_p(\omega, \theta) \quad (1)$$

in which,  $\theta$  denotes the direction of arrival of the incident wave mode,  $U(\omega)$  is the amplitude of the wave mode at angular frequency  $\omega$ ,  $H$  is a quantity associated with the material properties of the piezo-structure system,  $K_0$  indicates the wavenumber which characterizes the propagation, and  $D$  is the directivity function, which can be obtained as :

$$D_p(\omega, \theta) = \int_{\Omega_P} f(x)e^{-jk_0(\omega)\cdot x} d\Omega \quad (2)$$

where  $f(x)$  is the load distribution function, representing the transducer shape and polarization. Equation (2) is identified as the 2-D Fourier Transform (FT) of the function  $f(x)$ , allowing

one to estimate FT pairs and thus calculate directivity patterns corresponding to various transducer shapes. In other words, when designing a transducer for directional behavior, it is advantageous to first determine the desired directivity function in  $D$  and then use the FT to generate the corresponding transducer geometry that benefits such directional behavior.

The elasto-dynamic equations of motion which govern harmonic wave propagation within a plate-like structure can be described by this formula [6]:

$$\hat{u}(k, \omega) = \hat{P}^{-1}(k, \omega) \hat{f}(k, \omega) \quad (3)$$

where  $(\cdot)$  denotes the 2-D Fourier Transform from space  $x = [x_1, x_2]$  to wavenumber  $k = [k_1, k_2]$  domain, and  $u$  defines the plate displacement field in response to a load distribution  $f$  at frequency  $\omega$ , as determined by the differential operator  $P$  associated with the considered medium. According to [6], when  $\hat{P}(k, \omega) = 0$  the maximum displacement output can be attained where the load distribution intersects the medium's dispersion relation at wavenumber  $k^*$ , whose direction defines the direction of the generated wave in the plate. Thus, frequency-based beam steering is achieved through the design of the transducer load distribution  $\hat{f}(k, \omega)$ , i.e., its geometry, in a way that the direction of the generated waves can be controlled by varying the excitation frequency.

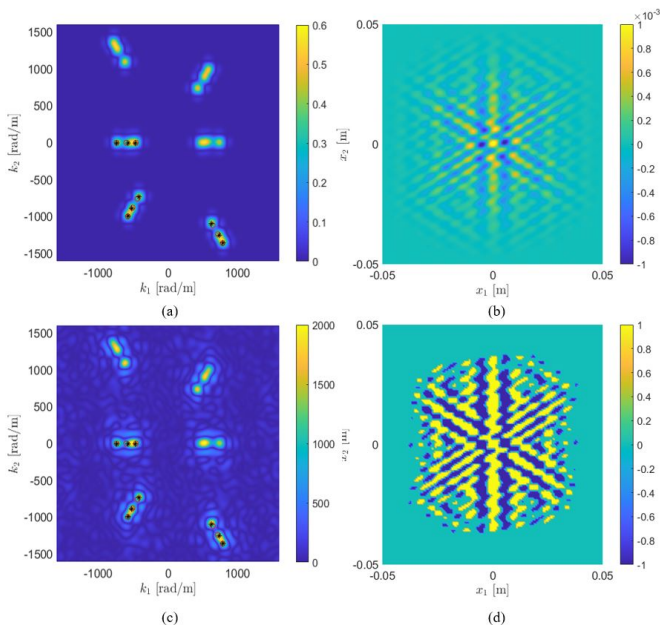


Fig. 1: FSAT design procedure: a) the load distribution in the wavenumber domain b) associated spatial distribution c) and d) effect of the quantization procedure on distributions (a) and (b)

In this paper, a discrete directivity function is considered for wave propagation at three different angles. As shown in Fig. 1a, the transducer is designed in the wavenumber domain first, considering three different excitation frequencies at each chosen direction. Although the corresponding geometry can be computed using the FT (Fig. 1b), such a geometry is

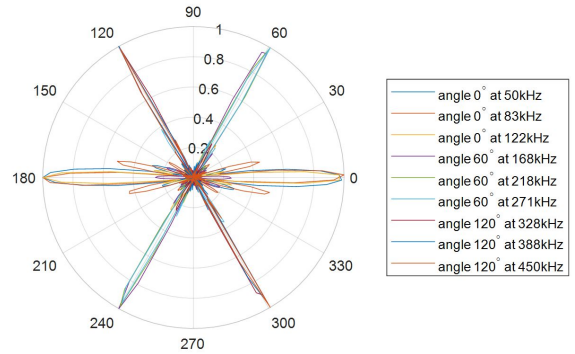


Fig. 2: Normalized directivity patterns at different frequencies.

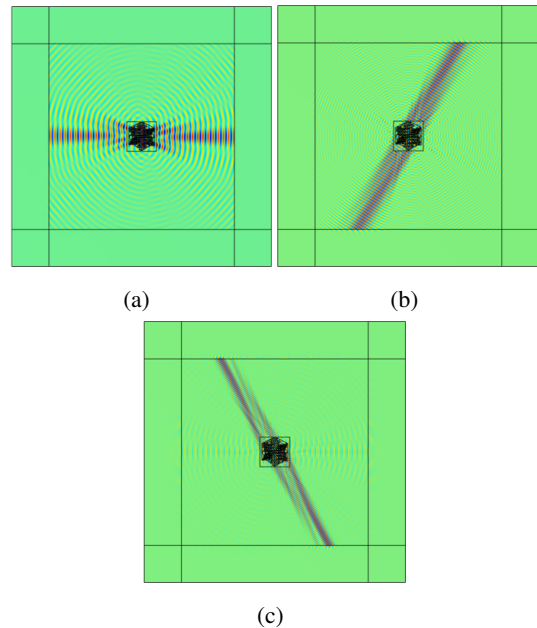


Fig. 3: Wavefields from Finite Element (FE) simulation at three different frequencies of 122 kHz, 168 kHz and 388 kHz propagating at 0°, 60°, and 120°, respectively.

practically unfeasible because it would need continuously modulated amplitude. To overcome this problem, the load distribution ( $f$ ) can be quantized using a specific threshold ( $\epsilon$ ) such that  $f$  is  $+1$  when  $f \geq \epsilon$ ,  $0$  when  $|f| < \epsilon$ , and  $-1$  for  $f \leq -\epsilon$ . Fig. 1d displays the final geometry after the quantization procedure.

The normalized radiation patterns corresponding to the directivity function described above are computed for the designed geometry, as shown in Fig. 2. Moreover, finite element (FE) simulation was carried out to verify the transducer performance. The simulation results in terms of the generated wavefield at three different frequencies are reported in Fig. 3, showing an excellent performance of the proposed device.

### III. QUADRATURE AMPLITUDE MODULATION

QAM is a modulation technique that modifies both the amplitude and the phase of the signal to be transmitted, while

holding the same carrier frequency  $F_c$  throughout time. Therefore, a proper choice of this latter parameter is of the utmost importance for GWs propagation, since numerous modes may be excited [1] depending on the operative frequency range. Therefore, a dedicated signal processing flow, based upon the four-step procedure in Fig. 4 and taking into consideration the dispersive behaviour of elastic waves, has been implemented to investigate the spatial multiplexing capabilities of FSATs when combined with this modulation technique. It comprises the following steps:

- 1) Step 1: *QAM coding and transmission*. In the first stage, QAM is used to map the digital sequence of bits into a number of symbols  $N_{sym}$  dictated by the selected number of binary digits; e.g., 16-QAM indicates that up to 16 different symbols can be generated if  $\log_2(16) = 4$  bits are used to represent a single piece of information. Every symbols is converted into a sinusoidal signal of identical frequency content but characterized by a specific amplitude  $A_n$  and phase  $\phi_n$  (step 1.a). In mathematical terms, one symbol reads as:

$$s_n(t) = A_n \cos(2\pi F_c t + \phi_n) = A_n e^{i(2\pi F_c t + \phi_n)} \quad (4)$$

which can be rewritten in an equivalent phasor form, yielding  $s_n = A_n e^{i\phi_n}$ . Both two formulations admit a geometrical interpretation in the complex plane, uniquely determined by two components (step 1.b): the in-phase component  $I_n$  lying on the real axis, and the in-quadrature component  $Q_n$  along the imaginary axis, with a phase shift of  $90^\circ$  between them. Such representation is also referred to as *constellation diagram*, owing to the fact that it represents all the possible complex-valued pairs of coordinates that a symbol can assume, i.e., it corresponds to the alphabet of binary values dictated by the selected number of digits per symbol. In the representative case depicted in Fig. 4, an 8-bit word  $b_n=0100111$  is considered: with 16-QAM, it is mapped into two symbols of four bits each (i.e., 0100 and 1111), corresponding to two different points of the constellation diagram.

After separation in its I/Q components, the symbol is ready to be “mounted” over the carrier by means of a sinusoidal signal (step 1.c): a cosine waveform for the in-phase component, namely  $s_{I_n}(t) = I_n \cos(2\pi F_c t)$ , and a sine waveform for the quadrature companion component, i.e.,  $s_{Q_n}(t) = Q_n \sin(2\pi F_c t)$ . These signals are then mixed together in a train of symbols  $s_n^{QAM}(t) = s_{I_n}(t) + s_{Q_n}(t)$ . After modulation, multiple modulated symbols can be combined in sequence and dispatched through the same channel forming the actuated signal  $s_n^{QAM}(t, 0)$ .

- 2) Step 2: *FSAT modelling*. GWs travel a communication distance  $d$  prior than reaching the receiver FSAT, whose frequency-steering effect has been modelled via a plane wave numerical model. The spectrum-based dispersion compensation mechanism in [10] has also been encompassed to maximize the quality of the demodulated

information: let’s call with  $s_n^{QAM}(t, d)$  the dispersion-compensated signal measured at the receiver side.

- 3) Step 3: *Reception and synchronization*. The exact instant for demodulation needs to be firstly retrieved at the receiving point. This can be easily achieved by cross-correlating the received message with a synchronization sequence  $s_{sym}(t)$  agreed in advance by the transmitter and the receiver.  $s_n^r(t)$  is used in step 3 of Fig. 4 to indicate the synchronized version of the received signal.
- 4) Step 4: *QAM decoding*. The synchronized message is then demodulated, again by resorting to the same sinusoidal signals in quadrature used at the encoding side, to separate the imaginary and real components  $s_{I_n}^r(t)$  and  $s_{Q_n}^r(t)$ . The high frequency content of the signal needs also to be removed by means of a low pass filter (LPF), returning the sought  $I^r$  and  $Q^r$ . These two latter quantities are plugged as input to the de-mapping block (performing the opposite operations entailed by the mapping block) and a reconstructed version of the bit chain,  $\hat{b}_n$ , is finally returned.

#### IV. NUMERICAL VALIDATION

The performances of the QAM protocol combined with the frequency steering capabilities of the designed FSAT device has been tested in a numerical setting consisting of a metallic plate (aluminum) of 1 m length and 1 mm thickness. Two devices were supposed to be located at the following positions (assuming the point (0,0) coinciding with the bottom left corner): Tx = (0.25, 0.25) and Rx = (0.75, 0.25), selected to communicate along the  $0^\circ$  direction at the specific frequencies of 50 kHz and 122 kHz compatible with the radiation pattern in Fig. 2. Three QAM-modulated symbols were transmitted at a symbol rate of 8000 bit/sym (corresponding to a bit rate of 24 and 32 kbits/s for 8 and 16-QAM, respectively), also simulating the effect of noise in the communication channel. The latter were chosen to be coincident with 20% and 50% of the actuated signal energy, resulting in a signal-to-noise ratio of 3 dB and 7 dB, correspondingly.

Results, which are illustrated in Fig. 5, were qualitatively evaluated by comparing the level of superimposition between the reconstructed and theoretically expected constellation diagrams, for different noise levels. As can be observed, the matching between the expected and the retrieved points remains always very high, independently from the QAM bit-width, the carrier frequency, and the noise value.

#### V. CONCLUSIONS

In this work, a new framework for GWs-based acoustic data communication built on the frequency steering functionalities of state-of-the-art FSAT transducers as enabling hardware for the realization of the QAM protocol has been proposed. Results related to the simulation of the transmission of three symbols over a metallic square plate demonstrates that the combination of this strategies can attain high communication rates and significant accuracy, paving the way to autonomous and cable-free communication systems.

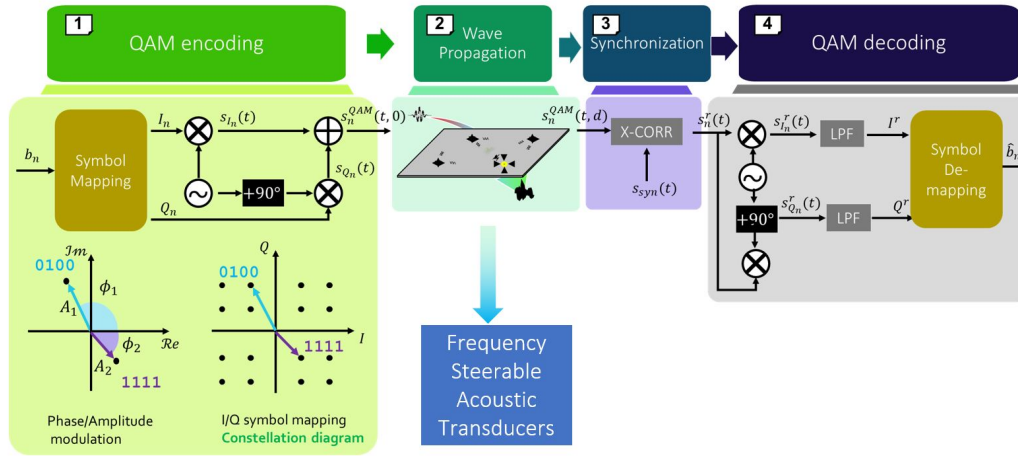


Fig. 4: Block diagram of the adopted QAM-based communication framework, specifically modelling the effects of wave dispersion.

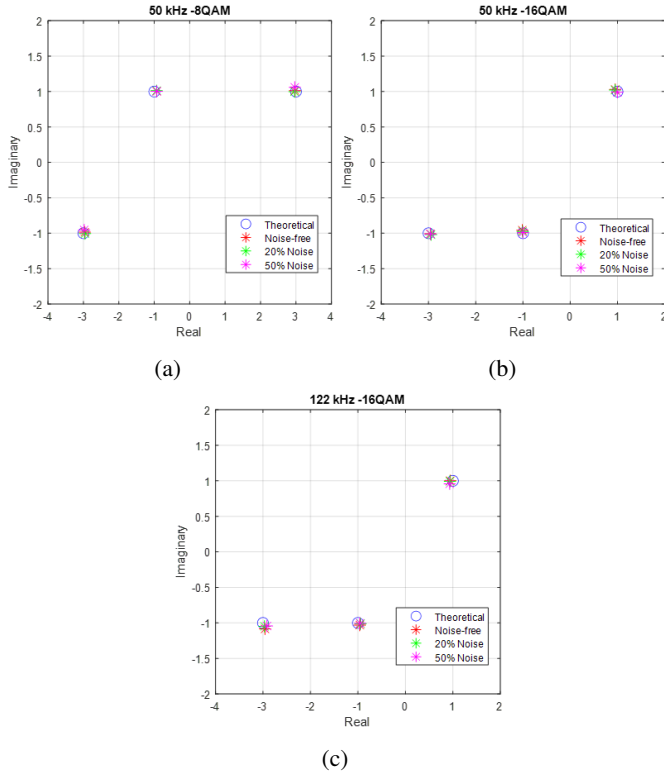


Fig. 5: Expected (blue, round) and reconstructed constellation diagrams under different channel noise levels: noise-free (red), 20% (green), 50% (magenta).

#### ACKNOWLEDGMENT

This work was carried out under the Guided Waves for Structural Health Monitoring (GW4SHM) project, funded by the Marie Skłodowska-Curie Actions Innovative Training Network, H2020 (Grant No. 860104). This project has received funding from the ECSEL Joint Undertaking (JU) under grant

agreement No 101007247. The JU receives support from the European Union's Horizon 2020 research and innovation programme and Finland, Germany, Ireland, Sweden, Italy, Austria, Iceland, Switzerland.

#### REFERENCES

- [1] Y. Sun, Y. Xu, W. Li, Q. Li, X. Ding, and W. Huang, "A lamb waves based ultrasonic system for the simultaneous data communication, defect inspection, and power transmission," *IEEE Transactions on Ultrasonics, Ferroelectrics, and Frequency Control*, pp. 1–1, 2021.
- [2] G. Trane, R. Mijarez, R. Guevara, and D. Pascacio, "Ppm-based system for guided waves communication through corrosion resistant multi-wire cables," *Physics Procedia*, vol. 70, pp. 672–675, 2015.
- [3] A. Heifetz, D. Shribak, X. Huang, B. Wang, J. Saniie, J. Young, S. Bakhtiari, and R. B. Vilim, "Transmission of images with ultrasonic elastic shear waves on a metallic pipe using amplitude shift keying protocol," *IEEE transactions on ultrasonics, ferroelectrics, and frequency control*, vol. 67, no. 6, pp. 1192–1200, 2020.
- [4] F. Zonzini, N. Testoni, A. Marzani, and L. De Marchi, "Low depth time reversal modulation technique for ultrasonic guided waves-based communications," in *2020 IEEE International Ultrasonics Symposium (IUS)*. IEEE, 2020, pp. 1–4.
- [5] X. Tang, S. Mandal, and T. Ozdemir, "A cmos soc for wireless ultrasonic power/data transfer and shm measurements on structures," *arXiv preprint arXiv:2110.12428*, 2021.
- [6] M. Mohammadgholiha, A. Palermo, N. Testoni, J. Moll, and L. De Marchi, "Finite element modeling and experimental characterization of piezoceramic frequency steerable acoustic transducers," *IEEE Sensors Journal*, vol. 22, no. 14, pp. 13958–13970, 2022.
- [7] M. Senesi, E. Baravelli, L. De Marchi, and M. Ruzzene, "Experimental demonstration of directional gw generation through wavenumber-spiral frequency steerable acoustic actuators," in *2012 IEEE International Ultrasonics Symposium*. IEEE, 2012, pp. 2694–2697.
- [8] O. A. Márquez Reyes, J. Moll, F. Zonzini, M. Mohammadgholiha, and L. De Marchi, "Quadrature amplitude modulation for acoustic data communication in ultrasonic structural health monitoring systems," in *2021 48th Annual Review of Progress in Quantitative Nondestructive Evaluation*. American Society of Mechanical Engineers Digital Collection, 2021.
- [9] M. Senesi and M. Ruzzene, "A frequency selective acoustic transducer for directional lamb wave sensing," *The Journal of the Acoustical Society of America*, vol. 130, no. 4, pp. 1899–1907, 2011.
- [10] F. Zonzini, L. De Marchi, N. Testoni, and A. Marzani, "Direct spread spectrum modulation and dispersion compensation for guided wave-based communication systems," in *2019 IEEE International Ultrasonics Symposium (IUS)*. IEEE, 2019, pp. 2500–2503.